Smooth Contact Between a Rigid Indenter and an Initially Stressed Orthotropic Beam

L. M. Keer* and R. Ballarini†
Northwestern University, Evanston, Illinois

The elastostatics problem of a rigid punch in smooth contact with an initially stressed transversely isotropic layer is investigated. The problem is formulated by writing the field equations in terms of suitable displacement potentials. In addition, an elementary beam theory solution is superimposed on the elasticity solution to satisfy the support boundary conditions for a finite beam. The cases studied are those of a simply supported beam and a clamped beam.

Nomenclature

c	= half of contact length
c_{ij}	= elastic stiffnesses
$\bar{e}(x)$	= load distribution in contact
h	= thickness of beam
ℓ	= length of beam
$M(x)$	= bending moment
P	= total vertical load
p	= load in direction of beam axis
R	= radius of curvature
v_x, v_z	= instantaneous velocity components parallel to and perpendicular to axis of beam (also v_1, v_3)
$\bar{v}_z$	= average value of v_z
x	= coordinate along axis of beam
z	= coordinate perpendicular to axis of beam
α	= constant related to initial stress
Δ, Δ_0	= deflection under centerline of punch
Λ	= load parameter
τ_{ab}	= first Piola-Kirchhoff stress
$\dot{\tau}^R_{ab}$	= relative incremental stress components
ν_1, ν_2	= roots of Eq. (14)

Introduction

SINCE elementary beam theory cannot account adequately for the local behavior in an elastic layer, it is hoped that through the present analysis a better understanding of such phenomena will develop. In a contact problem for a beam the local stress distributions as well as the global beam-type behavior must be properly understood. This is especially necessary for such materials as composites since they may be weak in certain directions. The understanding of both the global and local stresses is important to assess possible damage.

In practice composites may experience, in addition to the contact and support loadings, very large initial stresses. Thus, the theory to be developed in this paper will include materials in which a large initial stress can affect the overall response to the loading. To investigate such problems involving initial stress Hill[1] has given prominence to the nominal stress and its rate. Therefore, in the next section, an exact rate formulation is presented in terms of the rate of nominal or the first Piola-Kirchhoff stress, referred to and measured with respect to the current configuration. A similar approach was used by Dorris and Nemat-Nasser[2] in their study of the instability of a compressed layer on a half-space and by Keer et al.[3] in their study of the instability and splitting of compressed brittle elastic solids containing crack arrays. For an account of the theory of small deformations superimposed upon large ones, see Green et al.[4]

In the next section the basic equations are presented. The problem of an infinitely long, loaded layer is solved and, by matching the appropriate averaged boundary conditions at the supports with a suitable beam theory solution, a finite-beam solution is developed. The basic equations are reduced to Fredholm integral equations of the second kind which are solved by numerical methods. Stress distributions and compliances are obtained for various geometries, initial stress, and material properties. The results are compared with the predictions from beam theory as well as the Hertz solution for two bodies in contact.

Formulation

The considered problem is shown in Fig. 1, where a rigid punch is in smooth contact with an initially stressed, transversely isotropic beam. The plane strain theory used in this analysis is based upon small deformations superimposed upon a large uniform deformation; the small deformation accounts for the contact between the punch and the beam.

The stress components employed in this analysis are the first Piola-Kirchhoff stress τ^R_{ab}, with $\dot{\tau}^R_{ab}$ being the relative incremental stress components referred to the deformed, initially stressed state. In the absence of body forces the equations of equilibrium take on the form (see Biot,[5] Hill,[1] and Nemat-Nasser[6])

$$\dot{\tau}^R_{ab,a} = 0 \tag{1}$$

where a subscript preceded by a comma denotes partial differentiation with respect to the corresponding coordinate and where the repeated indices denote summation. The incremental stress boundary conditions are

$$\dot{\tau}^R_{ab} n_a = \dot{\tau}_b \tag{2}$$

where $\dot{\tau}_b$ are the components of prescribed incremental tractions referred to the initial stress state, and n_a are the components of the outward unit normal of the boundary.

Let $v_a(x,t)$ be the instantaneous velocity components of a typical material point in the current configuration; for the problem considered in this work v_a can be regarded as the incremental deformation. The deformation rate is defined as

$$D_{ab} = (v_{a,b} + v_{b,a})/2 \tag{3}$$

Presented at the ASME 103rd Winter Annual Meeting, Phoenix, Ariz., Nov. 14-19, 1982 as part of Symposium on Advances in Aerospace Structures and Materials, sponsored by the Aerospace Division of ASME. Received June 7, 1982; revision received Oct. 25, 1982.

*Professor, Department of Civil Engineering.
†Research Assistant, Department of Civil Engineering.

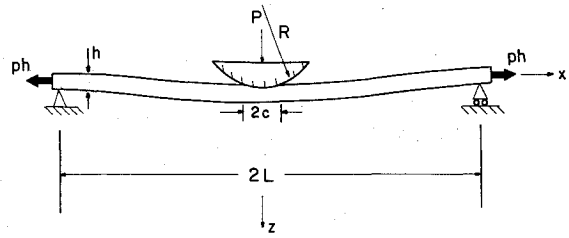

Fig. 1 Problem configuration (simple support case).

The stress rate $\dot{\tau}^R_{ab}$ is related to the deformation rate as follows:

$$\dot{\tau}^R_{ab} = \frac{D\tau_{ab}}{Dt} - D_{ac}\sigma_{cb} - D_{bc}\sigma_{ca} + v_{b,c}\sigma_{ca} \tag{4}$$

where $D\tau_{ab}/Dt$ denotes the Jaumann rate of the Kirchhoff stress and σ_{ab} are the components of the Cauchy stress. If we assume that for a transversely isotropic material the Jaumann rate of the Kirchhoff stress is given by[2]

$$\begin{aligned}
D\tau_{11}/Dt &= c_{11}v_{1,1} + c_{12}v_{2,2} + c_{13}v_{3,3}\\
D\tau_{22}/Dt &= c_{12}v_{1,1} + c_{11}v_{2,2} + c_{13}v_{3,3}\\
D\tau_{33}/Dt &= c_{13}(v_{1,1} + v_{2,2}) + c_{33}v_{3,3}\\
D\tau_{23}/Dt &= c_{44}(v_{2,3} + v_{3,2})\\
D\tau_{31}/Dt &= c_{44}(v_{3,1} + v_{1,3})\\
D\tau_{12}/Dt &= \tfrac{1}{2}(c_{11} - c_{12})(v_{2,1} + v_{1,2})
\end{aligned} \tag{5}$$

where c_{ij} are the elastic stiffnesses for a transversely isotropic material, then by treating σ_{ab} in Eq. (4) as an initial stress and assuming plane strain conditions ($v_2 = 0$, $\partial/\partial x_2 = 0$) the basic equations for the problem with constant tensile stress p in the x_1 direction are

$$\begin{aligned}
\dot{\tau}^R_{11} &= (c_{11} - p)v_{1,1} + c_{13}v_{3,3}\\
\dot{\tau}^R_{22} &= c_{12}v_{1,1} + c_{13}v_{3,3}\\
\dot{\tau}^R_{33} &= c_{13}v_{1,1} + c_{33}v_{3,3}\\
\dot{\tau}^R_{13} &= (c_{44} + p/2)v_{3,1} + (c_{44} - p/2)v_{1,3}\\
\dot{\tau}^R_{31} &= (c_{44} - p/2)(v_{3,1} + v_{1,3})\\
\dot{\tau}^R_{12} &= \dot{\tau}^R_{21} = \dot{\tau}^R_{23} = \dot{\tau}^R_{32} = 0
\end{aligned} \tag{6}$$

Boundary Conditions

The boundary conditions for the problem shown in Fig. 1 are

$$\begin{aligned}
&\dot{\tau}^R_{31} = 0 && z = 0 && -\infty < x < \infty\\
&\dot{\tau}^R_{33} = 0 && z = 0 && c < |x| < \infty\\
&\dot{\tau}^R_{31} = \dot{\tau}^R_{33} = 0 && z = h && -\infty < x < \infty\\
&v_3 = \Delta - x^2/2R && z = 0 && -c \le x \le c
\end{aligned} \tag{7}$$

where R is the radius of curvature of the indenter and Δ the displacement at (0,0). In addition, at the support, the following conditions must be satisfied:

1) Simply supported beam

$$M(L) = 0, \qquad \bar{v}_z(L) = 0 \tag{8}$$

where $M(x)$ is the bending moment at x and $\bar{v}_z(x)$ is the average value of the deflection at x. (At $x = L$ the average displacement is approximately the pointwise displacement.)

2) Clamped beam

$$\bar{v}_z(L) = 0, \qquad \partial\bar{v}_z(L)/\partial x = 0 \tag{9}$$

where

$$\frac{\partial\bar{v}_z}{\partial x} = \frac{1}{h}\int_0^h \frac{\partial v_z}{\partial x}\,dz \tag{10}$$

is the average slope at x.

Layer Solution

Defining potentials as

$$v_1 = \phi_{,1}, \qquad v_3 = k\phi_{,3} \tag{11}$$

where k is a constant to be determined leads to (see Ref. 7)

$$\begin{aligned}
&(c_{11} - p)\phi_{,11} + [k(c_{13} + c_{44} - p/2) + c_{44} - p/2]\phi_{,33} = 0\\
&[k(c_{44} + p/2) + c_{13} + c_{44} - p/2]\phi_{,11} + kc_{33}\phi_{,33} = 0
\end{aligned} \tag{12}$$

and hence

$$\frac{k(c_{13} + c_{44} - p/2) + c_{44} - p/2}{c_{11} - p} = \frac{kc_{33}}{k(c_{44} + p/2) + c_{13} + c_{44} - p/2} = \nu \tag{13}$$

or equivalently

$$\begin{aligned}
&(c_{11} - p)(c_{44} + p/2)\nu^2 + [c_{13}(2c_{44} + c_{13}) + p^2/2\\
&\quad - p(c_{13} + c_{44} - c_{33}) - c_{11}c_{33}]\nu + (c_{44} - p/2)c_{33} = 0
\end{aligned} \tag{14}$$

There will be potential functions, ϕ_i, $i = 1,2$, implied by the two roots for ν in Eq. (14).

The following potentials satisfy Eq. (12) and are associated with a layer loaded only on its *top surface* in terms of the Fourier transform $d(\xi)$:

$$\begin{aligned}
\phi_1 &= -\frac{c_2}{c_1}\int_0^\infty \left\{\frac{K_1(\xi h)}{K_2(\xi h)}\sinh\left(\frac{\xi z}{\sqrt{\nu_1}}\right)\right.\\
&\quad \left. - \frac{K_3(\xi h)}{K_2(\xi h)}\cosh\left(\frac{\xi z}{\sqrt{\nu_1}}\right)\right\} d(\xi)\cos(\xi x)\,d\xi\\
\phi_2 &= \int_0^\infty \left\{\frac{K_1(\xi h)}{K_2(\xi h)}\sinh\left(\frac{\xi z}{\sqrt{\nu_2}}\right)\right.\\
&\quad \left. + \cosh\left(\frac{\xi z}{\sqrt{\nu_2}}\right)\right\} d(\xi)\cos(\xi x)\,d\xi
\end{aligned} \tag{15}$$

where

$$\begin{aligned}
K_1(\xi h) &= \frac{c_4 c_1}{c_3 c_2}\sinh\left(\frac{\xi h}{\sqrt{\nu_1}}\right)\cosh\left(\frac{\xi h}{\sqrt{\nu_2}}\right)\\
&\quad - \sinh\left(\frac{\xi h}{\sqrt{\nu_2}}\right)\cosh\left(\frac{\xi h}{\sqrt{\nu_1}}\right)\\
K_2(\xi h) &= \cosh\left(\frac{\xi h}{\sqrt{\nu_2}}\right)\cosh\left(\frac{\xi h}{\sqrt{\nu_1}}\right)\\
&\quad - \frac{c_4 c_1}{c_3 c_2}\sinh\left(\frac{\xi h}{\sqrt{\nu_2}}\right)\sinh\left(\frac{\xi h}{\sqrt{\nu_1}}\right) - 1
\end{aligned}$$

$$K_3(\xi h)=\frac{c_4c_1}{c_3c_2}\cosh\left(\frac{\xi h}{\sqrt{\nu_1}}\right)\cosh\left(\frac{\xi h}{\sqrt{\nu_2}}\right)$$
$$-\sinh\left(\frac{\xi h}{\sqrt{\nu_1}}\right)\sinh\left(\frac{\xi h}{\sqrt{\nu_2}}\right)-\frac{c_4c_1}{c_3c_2} \tag{16}$$

and

$$c_1=(1+k_1)/\sqrt{\nu_1}, \qquad c_2=(1+k_2)/\sqrt{\nu_2}$$
$$c_3=(k_1c_{33}-\nu_1c_{13})/\nu_1, \quad c_4=(k_2c_{33}-\nu_2c_{13})/\nu_2 \tag{17}$$

Beam Theory

By using the equations for a transversely isotropic material with initial stress the usual beam theory equations can be easily derived for plane strain. This solution will have the form

$$v_z(x)=C+Dx+A\sinh(\alpha x)+B\cosh(\alpha x) \tag{18}$$

where

$$\alpha^2=12ph/h^3(c_{11}-p-c_{13}^2/c_{33}) \tag{19}$$

The bending moment is given by

$$M(x)=-\frac{h^3}{12}\left(c_{11}-p-\frac{c_{13}^2}{c_{33}}\right)\frac{\mathrm{d}^2\bar{v}_z}{\mathrm{d}x^2} \tag{20}$$

and the relation between shear and bending moment is

$$V=\frac{\mathrm{d}M}{\mathrm{d}x}+ph\frac{\mathrm{d}\bar{v}_z}{\mathrm{d}x} \tag{21}$$

In the case of a constant moment M applied at $x=\pm L$ the solution for $\bar{v}_z$ is

$$\bar{v}_z=B\cosh(\alpha x)+M/ph \tag{22}$$

Equilibrium Relations

To show the equilibrium relations, the normal stresses are integrated along the contact length. On $z=0$,

$$\dot{\tau}_{33}^R=\int_0^\infty E(\xi)\cos(\xi x)\,\mathrm{d}\xi \tag{23}$$

where

$$E(\xi)=\xi^2\mathrm{d}(\xi)\frac{K_4(\xi h)}{K_2(\xi h)} \tag{24}$$

and

$$K_4(\xi h)=2c_4\cosh\left(\frac{\xi h}{\sqrt{\nu_2}}\right)\cosh\left(\frac{\xi h}{\sqrt{\nu_1}}\right)$$
$$-\left(\frac{c_3^2c_2^2+c_1^2c_4^2}{c_1c_2c_3}\right)\sinh\left(\frac{\xi h}{\sqrt{\nu_2}}\right)\sinh\left(\frac{\xi h}{\sqrt{\nu_1}}\right)-2c_4 \tag{25}$$

Inverting Eq. (23),

$$E(\xi)=2/\pi\int_0^c\tilde{e}(x)\cos(\xi x)\,\mathrm{d}x \tag{26}$$

where

$$\tilde{e}(x)=\dot{\tau}_{33}^R(x,0) \tag{27}$$

Since the problem is symmetric in x, $\tilde{e}(x)=\tilde{e}(-x)$, and the total load is given in terms of the normal stresses as

$$P=-\int_{-c}^{c}\tilde{e}(x)\,\mathrm{d}x \tag{28}$$

If the two faces of the layer at points x and $-x$ are cut and the shear stresses are integrated, the result should equal the total load P. After some manipulation, using Eqs. (23) and (26), it can be shown that

$$V=\int_0^h\dot{\tau}_{13}^R\mathrm{d}z=\frac{1}{2}\int_{-c}^{c}\tilde{e}(t)\,\mathrm{d}t \tag{29}$$

Summing the forces in the vertical direction

$$P+2\int_0^h\dot{\tau}_{13}^R\mathrm{d}z=0 \tag{30}$$

It can be shown that on any section of the layer

$$\int_0^h\dot{\tau}_{11}^R\mathrm{d}z=0 \tag{31}$$

The moment at any section is given as

$$M(x)=\int_0^\infty\mathrm{d}(\xi)\frac{K_5(\xi h)}{K_2(\xi h)}\cos(\xi x)\,\mathrm{d}\xi \tag{32}$$

where

$$K_5(\xi h)=(c_6\nu_2-c_5c_4\nu_1/c_3)[\cosh(\xi h/\sqrt{\nu_1})-\cosh(\xi h/\sqrt{\nu_2})]$$
$$+(c_2c_5\nu_1/c_1+c_4c_1c_6\nu_2/c_3c_2)\sinh(\xi h/\sqrt{\nu_2})\sinh(\xi h/\sqrt{\nu_1})$$
$$+(c_6\nu_2+c_4c_5\nu_1/c_3)[1-\cosh(\xi h/\sqrt{\nu_2})\cosh(\xi h/\sqrt{\nu_1})] \tag{33}$$

and

$$c_5=c_{11}-p-c_{13}k_1/\nu_1, \quad c_6=c_{11}-p-c_{13}k_2/\nu_2 \tag{34}$$

If an average value of the slope $\partial\bar{v}_z/\partial x$ is taken, then the relation

$$ph\overline{\frac{\partial v_z}{\partial x}}=p\int_0^\infty\xi\mathrm{d}(\xi)\frac{K_6(\xi h)}{K_2(\xi h)}\sin(\xi x)\,\mathrm{d}\xi \tag{35}$$

is obtained, where

$$K_6(\xi h)=(c_4k_1/c_3-k_2)[\cosh(\xi h/\sqrt{\nu_1})-\cosh(\xi h/\sqrt{\nu_2})]$$
$$+(k_2+c_4k_1/c_3)[\cosh(\xi h/\sqrt{\nu_2})\cosh(\xi h/\sqrt{\nu_1})-1]$$
$$-(k_1c_2/c_1+k_2c_1c_4/c_3c_2)\sinh(\xi h/\sqrt{\nu_2})\sinh(\xi h/\sqrt{\nu_1}) \tag{36}$$

Using Eqs. (29), (32), and (35) it can be shown that

$$V=\frac{\mathrm{d}M}{\mathrm{d}x}+ph\overline{\frac{\partial v_z}{\partial x}} \tag{37}$$

which is the well-known beam column equation.

Boundary Value Problem

The problem is now reduced to a set of dual integral equations. On $z=0$

$$\dot{\tau}_{33}^R=\int_0^\infty E(\xi)\cos(\xi x)\,\mathrm{d}\xi=0, \quad x>c \tag{38}$$

$$\frac{\partial v_z}{\partial x} = \frac{k_1 - k_2}{(1+k_1)\sqrt{\nu_2}} \int_0^\infty \frac{K_1(\xi h)}{K_4(\xi h)} E(\xi)\sin(\xi x)\,d\xi = -x/R \qquad 0 \le x \le c$$

If $E(\xi)$ is defined as

$$E(\xi) = \int_0^c J_0(\xi t)\psi(t)\,dt \tag{39}$$

and substituted into the first of Eqs. (38)

$$\dot{\tau}_{33}^R = \int_x^c \frac{\psi(t)}{\sqrt{t^2 - x^2}}\,dt, \qquad 0 \le x \le c$$

$$= 0, \qquad x > c \tag{40}$$

and the first of Eqs. (38) is satisfied automatically. On $z = 0$,

$$v_z = \frac{k_2 - k_1}{(1+k_1)\sqrt{\nu_2}} \int_0^c \psi(t) \left\{ \int_0^\infty J_0(\xi t) \frac{K_1(\xi h)}{K_4(\xi h)} \frac{\cos(\xi x)}{\xi}\,d\xi \right\} dt \tag{41}$$

It can be shown that this integral diverges. The physical meaning is that the layer is infinite in the x direction and any load will produce an infinite deflection. To introduce the finiteness of the layer at $x = \pm L$ a beam bending solution is superimposed on the elasticity solution to satisfy simply supported and clamped boundary conditions.

Simply Supported Beam

For a simply supported beam the moment and vertical deflection at the supports are zero. Remembering Eq. (24) and substituting Eq. (39) into Eq. (32), at $x = L$

$$M(L) = \int_0^c \psi_s(t) \left\{ \int_0^\infty J_0(\xi t) \frac{K_5(\xi h)}{K_4(\xi h)} \frac{\cos(\xi L)}{\xi^2}\,d\xi \right\} dt$$

$$- phB\cosh(\alpha L) = 0 \tag{42}$$

where $-phB\cosh(\alpha L)$ is an elementary beam bending solution and ψ_s the auxiliary function for the simply supported case. Solving for B in Eq. (42), the deflection on $z = 0$ becomes

$$v_z = \frac{k_2 - k_1}{(1+k_1)\sqrt{\nu_2}} \int_0^c \psi_s(t) \left\{ \int_0^\infty J_0(\xi t) \frac{K_1(\xi h)}{K_4(\xi h)} \frac{\cos(\xi x)}{\xi}\,d\xi \right\} dt$$

$$+ \frac{\cosh(\alpha x)}{ph\cosh(\alpha L)} \int_0^c \psi_s(t) \left\{ \int_0^\infty J_0(\xi t) \frac{K_5(\xi h)}{K_4(\xi h)} \frac{\cos(\xi L)}{\xi^2}\,d\xi \right\} dt$$

$$+ M/ph \tag{43}$$

where M/ph is an elementary beam bending solution. Differentiating Eq. (43) we get

$$\frac{\partial v_z}{\partial x} = \frac{k_1 - k_2}{(1+k_1)\sqrt{\nu_2}} \int_0^c \psi_s(t) \left\{ \int_0^\infty J_0(\xi t) \frac{K_1(\xi h)}{K_4(\xi h)} \sin(\xi x)\,d\xi \right\} dt$$

$$+ \frac{\alpha\sinh(\alpha x)}{ph\cosh(\alpha L)} \int_0^c \psi_s(t) \left\{ \int_0^\infty J_0(\xi t) \frac{K_5(\xi h)}{K_4(\xi h)} \frac{\cos(\xi L)}{\xi^2}\,d\xi \right\} dt \tag{44}$$

It is noted that when the initial stress p becomes zero, by taking the proper limits and expanding the hyperbolic and trigonometric functions about $\xi = 0$, the integrand of the kernel of the elasticity solution diverges. However, the added elementary solution removes the divergent part of the integrand, hence the integral is well behaved. By expanding the functions as $\xi \to \infty$ the integrand in the elasticity solution approaches the value $c_7 J_0(\xi t)\sin(\xi x)$, where

$$c_7 = \frac{(k_2 - k_1)\sqrt{\nu_1}\sqrt{\nu_2}}{(k_2 c_{33} - \nu_2 c_{13})(1+k_1)\sqrt{\nu_1} - (k_1 c_{33} - \nu_1 c_{13})(1+k_2)\sqrt{\nu_2}} \tag{45}$$

To help the convergence at the upper limit this term is added and subtracted from the integrand and a part of the integral is evaluated in closed form. Then write

$$\frac{\partial v_z}{\partial x} = \int_0^c \psi_s(t)\bar{K}(x,t)\,dt + c_7 \int_0^x \frac{\psi_s(t)\,dt}{\sqrt{x^2 - t^2}} \tag{46}$$

where

$$\bar{K}(x,t) = \int_0^\infty \left\{ \frac{k_1 - k_2}{(1+k_1)\sqrt{\nu_2}} \left(\frac{K_1(\xi h)}{K_4(\xi h)} + \frac{c_1}{c_4 c_1 - c_3 c_2} \right) \sin(\xi x) \right.$$

$$\left. + \frac{\alpha\sinh(\alpha x) K_5(\xi h)\cos(\xi L)}{ph\cosh(\alpha L) K_4(\xi h)\xi^2} \right\} J_0(\xi t)\,d\xi \tag{47}$$

where

$$\frac{\partial v_z}{\partial x} = -\frac{x}{R} \qquad |x| \le c \tag{48}$$

Multiplying both sides of Eq. (46) by

$$\int_0^s \frac{x\,dx}{\sqrt{s^2 - x^2}}$$

and evaluating the integrals leads to

$$\frac{s}{R} = c_7\psi_s(s) + s\int_0^c \psi_s(t)K(s,t)\,dt \tag{49}$$

where

$$K(s,t) = \int_0^\infty \left\{ \frac{(k_2 - k_1)K_1(\xi h)}{(1+k_1)\sqrt{\nu_2}K_4(\xi h)} \xi J_0(\xi s) - c_7 \xi J_0(\xi s) \right.$$

$$\left. - \frac{12 I_0(\alpha s) K_5(\xi h)\cos(\xi L)}{h^3 (c_{11} - p - c_{13}^2/c_{33})\cosh(\alpha L) K_4(\xi h)\xi^2} \right\} J_0(\xi t)\,d\xi \tag{50}$$

Equation (49) is nondimensionalized by making the substitutions $\beta = \xi h$, $t = cu$, $s = cr$, $\lambda = c/h$, $\alpha^* = \alpha h$, and $\psi_s(cr) = cr c_{44}\hat{\psi}_s(r)/R$. The following Fredholm integral equation of the second kind is obtained:

$$\hat{\psi}_s(r) = 1/c_7 c_{44} - \lambda^2 \int_0^1 u\hat{\psi}_s(u)\hat{K}(cr,cu)\,du \tag{51}$$

where

$$\hat{K}(cr,cu) = \int_0^\infty \left\{ \frac{(k_2 - k_1)K_1(\beta)\beta J_0(\beta\lambda r)}{(1+k_1)\sqrt{\nu_2}c_7 K_4(\beta)} - \beta J_0(\beta\lambda r) \right.$$

$$\left. - \frac{12 I_0(\alpha^*\lambda r)\cos(\beta L/h) K_5(\beta)}{(c_{11} - p - c_{13}^2 c_{33}) c_7 \cosh(\alpha^* L/h)\beta^2 K_4(\beta)} \right\} J_0(\beta\lambda u)\,d\beta \tag{52}$$

Recalling Eq. (40), on $z = 0$

$$\dot{\tau}_{33}^R = cc_{44}/R \int_r^1 \frac{u\hat{\psi}_s(u)\,du}{\sqrt{u^2 - r^2}} \tag{53}$$

Having solved for discrete values of $\hat{\psi}_s(u)$, the integration in Eq. (53) is performed by approximating $\hat{\psi}_s(u)$ with a polynomial and solving the integral in closed form. The total load is given as

$$P=2\int_0^c \dot{\tau}_{33}^R \mathrm{d}x = c_{44}\pi c^2/R\int_0^1 u\hat{\psi}_s(u)\,\mathrm{d}u \tag{54}$$

and this integral is also solved numerically.

For a simply supported beam the deflection of the supports is zero. From Eq. (43) we can solve for M/ph, and the deflection at (0,0) becomes

$$\Delta=\int_0^c \psi_s(t)\,\mathrm{d}t\int_0^\infty\left\{\frac{(k_2-k_1)K_1(\xi h)}{(1+k_1)\sqrt{\nu_2}K_4(\xi h)}\left(\frac{1-\cos(\xi L)}{\xi}\right)\right.$$
$$\left.+\frac{\cos(\xi L)K_5(\xi h)}{ph\xi^2K_4(\xi h)}\left(\frac{1}{\cosh(\alpha L)}-1\right)\right\}J_0(\xi t)\,\mathrm{d}\xi \tag{55}$$

To enhance the convergence at the upper limit, we add and subtract the term $c_7(1-\cos(\xi L))/\xi$. We can solve part of this integral in closed form. By nondimensionalizing, the result is

$$\Delta=c^2/R\int_0^1 u\hat{\psi}_s(u)\left\{\int_0^\infty\left[\frac{(k_2-k_1)c_{44}}{(1+k_1)\sqrt{\nu_2}}\left(\frac{K_1(\beta)}{K_4(\beta)}\right.\right.\right.$$
$$\left.-\frac{c_7(1+k_1)\sqrt{\nu_2}}{(k_2-k_1)}\right)\left(\frac{1-\cos(\beta L/h)}{\beta}\right)$$
$$\left.+\frac{c_{44}\cos(\beta L/h)K_5(\beta)}{p\beta^2K_4(\beta)}\left(\frac{1}{\cosh(\alpha^* L/h)}-1\right)\right]$$
$$\left.\times J_0(\beta\lambda u)\,\mathrm{d}\beta+c_7c_{44}\operatorname{arch}(L/cu)\right\}\mathrm{d}u \tag{56}$$

The Hertz solution can be extracted from Eq. (51) by making $c/h \ll 1$. The result is

$$\hat{\psi}_s(r)=1/c_7c_{44}\quad \dot{\tau}_{33}^R=c\sqrt{1-r^2}/c_7R\quad P=\pi c^2/2c_7R \tag{57}$$

Clamped Ends

The next case is that of a beam with clamped ends. Using Eq. (35) and the second of the boundary conditions [Eqs. (9)], at $x=L$

$$\frac{1}{h}\int_0^\infty \frac{\xi\,\mathrm{d}(\xi)}{K_2(\xi h)}K_6(\xi h)\sin(\xi L)+B\alpha\sinh(\alpha L)=0 \tag{58}$$

where $B\alpha\sinh(\alpha L)$ is an elementary beam bending solution. From Eq. (58) we determine B and on $z=0$ we get

$$\frac{\partial v_z}{\partial x}=\frac{(k_1-k_2)}{(1+k_1)\sqrt{\nu_2}}\int_0^c\psi_c(t)\,\mathrm{d}t\int_0^\infty\frac{J_0(\xi t)K_1(\xi h)\sin(\xi x)}{K_4(\xi h)}\mathrm{d}\xi$$
$$-\frac{\sinh(\alpha x)}{h\sinh(\alpha L)}\int_0^c\psi_c(t)\,\mathrm{d}t\int_0^\infty\frac{J_0(\xi t)K_6(\xi h)\sin(\xi L)}{\xi K_4(\xi h)}\mathrm{d}\xi \tag{59}$$

where ψ_c is the auxiliary function for the clamped case. Using the same procedure as for the simply supported case we get

$$\hat{\psi}_c(r)=1/c_7c_{44}-\lambda^2\int_0^1 u\hat{\psi}_c(u)\hat{K}(cr,cu)\,\mathrm{d}u \tag{60}$$

where

$$\hat{K}(cr,cu)=\int_0^\infty\left[\frac{(k_2-k_1)K_1(\beta)\beta J_0(\beta\lambda r)}{(1+k_1)\sqrt{\nu_2}c_7K_4(\beta)}-\beta J_0(\beta\lambda r)\right.$$
$$\left.+\frac{\alpha^*\sin(\beta L/h)I_0(\alpha^*\lambda r)K_6(\beta)}{\sinh(\alpha^*L/h)\beta K_4(\beta)}\right]J_0(\beta\lambda u)\,\mathrm{d}\beta \tag{61}$$

To solve for the displacement under the indenter we make use of the first of Eqs. (9) and solve for M/ph. We then get

$$\Delta=c^2/R\int_0^1 u\hat{\psi}_c(u)\left\{\int_0^\infty\left[\frac{(k_2-k_1)c_{44}}{(1+k_1)\sqrt{\nu_2}}\left(\frac{K_1(\beta)}{K_4(\beta)}\right.\right.\right.$$
$$\left.-\frac{c_7(1+k_1)\sqrt{\nu_2}}{(k_2-k_1)}\right)\left(\frac{1-\cos(\beta L/h)}{\beta}\right)$$
$$\left.+\frac{c_{44}\sin(\beta L/h)[\cosh(\alpha^* L/h)-1]K_6(\beta)}{\alpha^*\beta\sinh(\alpha^* L/h)K_4(\beta)}\right]J_0(\beta\lambda u)\,\mathrm{d}\beta$$
$$\left.+c_7c_{44}\operatorname{arch}(L/cu)\right\}\mathrm{d}u \tag{62}$$

Numerical Results and Conclusions

The integration in Eqs. (51), (56), (60), and (62) was performed numerically using a Gaussian quadrature scheme. The parameters L/h, c/h, p, and elastic moduli were varied to study the effects of various loading conditions, beam geometries, initial stress, and material properties. Two transversely isotropic materials were chosen for this investigation. The first, magnesium, is nearly isotropic, and to investigate the effect of more severe anisotropy, cadmium was chosen. The elastic moduli of both materials were obtained from Ref. 8 and are listed in Table 1.

Certain dimensionless parameters are defined as:

$$\Delta_0=\Delta R/\ell^2 \quad \text{(deflection under centerline of punch)}$$

$$\Lambda=12P\ell R/h^3(c_{11}-p-c_{13}^2/c_{33}) \quad \text{(load parameter)}$$

$$\sigma^*=\dot{\tau}_{33}^R c/P \quad \text{(stress parameter)}$$

$$C/C^*=\Lambda_{\text{beam theory}}/\Lambda_{\text{elasticity theory}}$$

Initial Stress Zero

To investigate the effect of anisotropy the results for $p=0$ are first studied. Figures 2 and 3 are load deflection curves for the simply supported condition. Since the load parameter eliminates the bending stiffness, it can be seen that magnesium and cadmium differ slightly in their load deflection behavior. Although it cannot be observed from the graphs, the numerical results show that cadmium does experience larger deflections for the same load. This is due to the fact that cadmium is softer in the transverse direction and is therefore more sensitive to the contact. The effect is more pronounced as the aspect ratio decreases and the contact length increases. The deflection in these cases is due to the punch penetrating into the material and, since cadmium is softer in the transverse direction, it experiences larger deflections. When the aspect ratio is increased, the deflection is mostly due to bending and this softness does not manifest itself as much. Figures 4 and 5 show that beam theory is more than adequate for determining the global behavior of the beam. Since the system constraint for beam theory is greater, beam theory predicts a stiffer beam. To examine contact stress distributions, only one aspect ratio and one end con-

Table 1 Elastic moduli for magnesium and cadmium, $\times 10^{10}$ N/m^2

	Magnesium	Cadmium
c_{11}	5.857	10.92
c_{12}	2.501	3.976
c_{13}	2.079	3.754
c_{33}	6.110	4.602
c_{44}	1.658	1.562

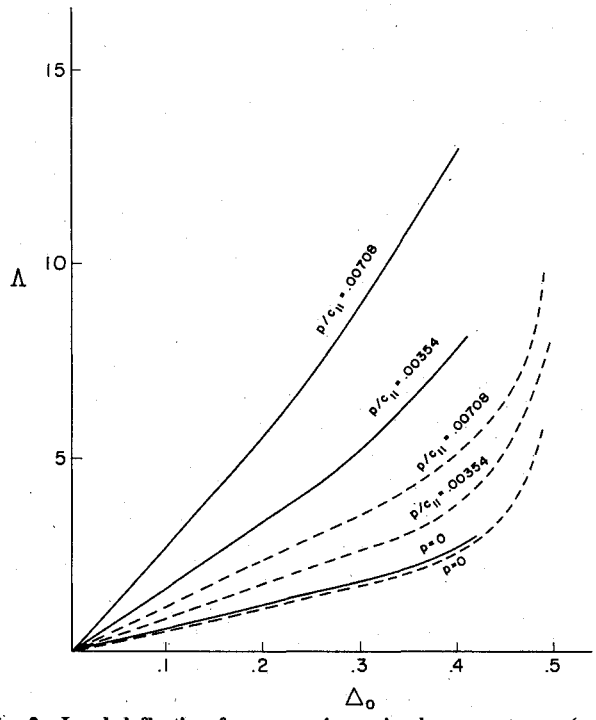

Fig. 2 Load deflection for magnesium, simple support case (solid line is $L/h = 10.0$, dashed line $L/h = 5.0$).

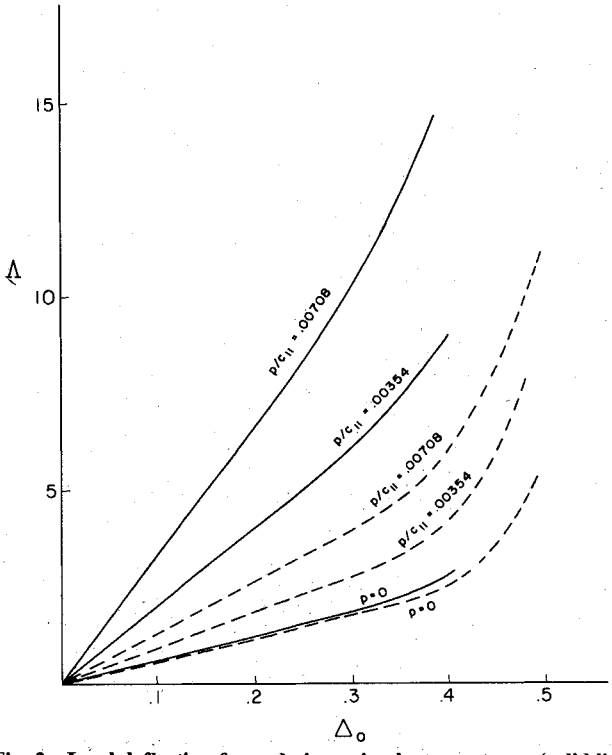

Fig. 3 Load deflection for cadmium, simple support case (solid line is $L/h = 10.0$, dashed line $L/h = 5.0$).

dition was necessary for each material, since this distribution has been found to be invariant with respect to end conditions and aspect ratios when the initial stress is zero and is a function of c/h only. (See Figs. 6 and 7.) For small values of c/h, the distribution is almost identical to the Hertz solution [Eq. (57)], but as c/h increases, the results change dramatically. From beam theory zero normal stresses are predicted along the contact region except for concentrated loads equal to $P/2$ at $x = \pm c$. As the contact length increases, the elasticity

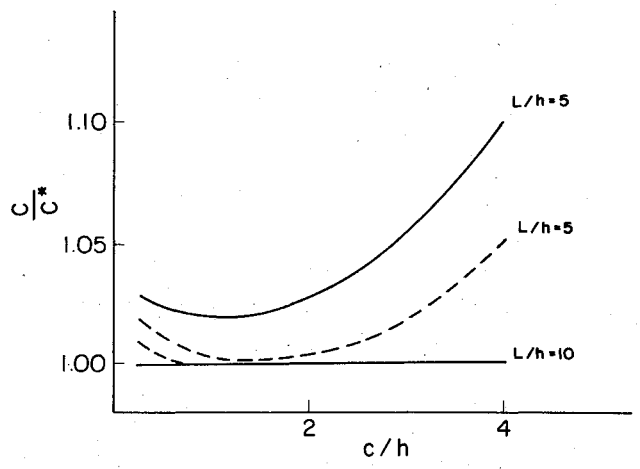

Fig. 4 Ratio of elasticity solution compliance to beam theory solution compliance for magnesium, simple support (solid line is $p = 0$, dashed line $p/c_{11} = 0.00718$).

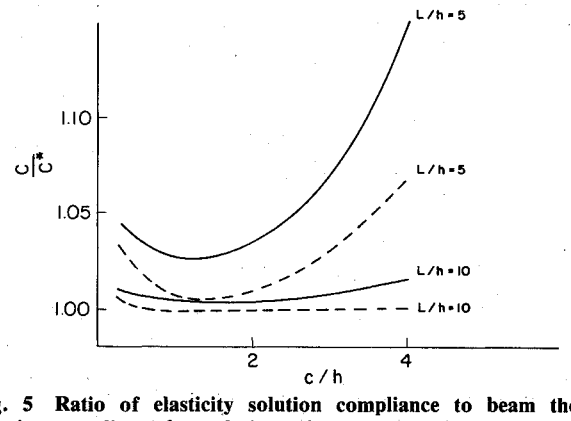

Fig. 5 Ratio of elasticity solution compliance to beam theory solution compliance for cadmium, simple support (solid line is $p = 0$, dashed line $p/c_{11} = 0.00708$).

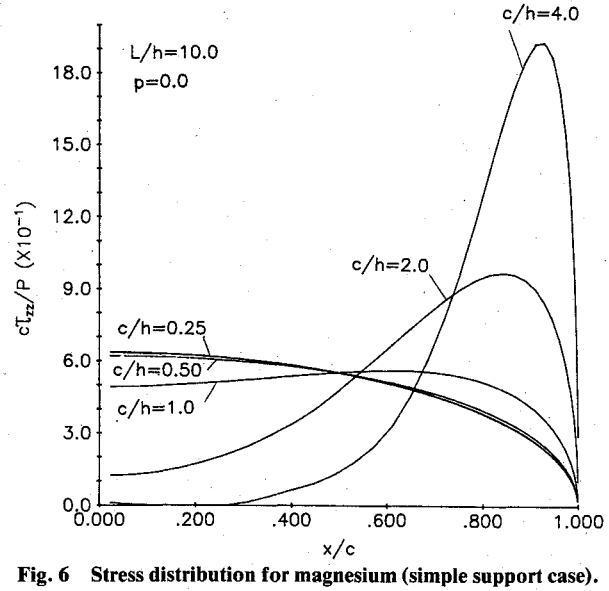

Fig. 6 Stress distribution for magnesium (simple support case).

solution is expected to approach this simple theory solution and, as seen from these plots, it does.

An interesting result is noticed from these distributions. Magnesium experiences higher peak stresses than cadmium for large contact lengths. The anisotropy manifests itself in the stresses through the distribution of these stresses. These distributions must be properly understood in order to make

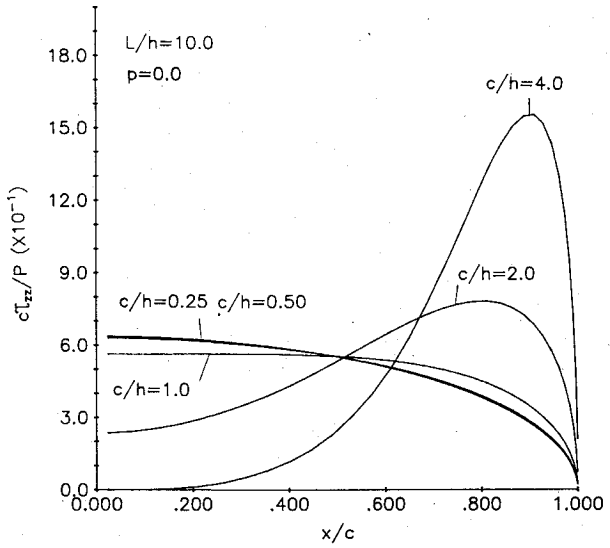

Fig. 7 Stress distribution for cadmium (simple support case).

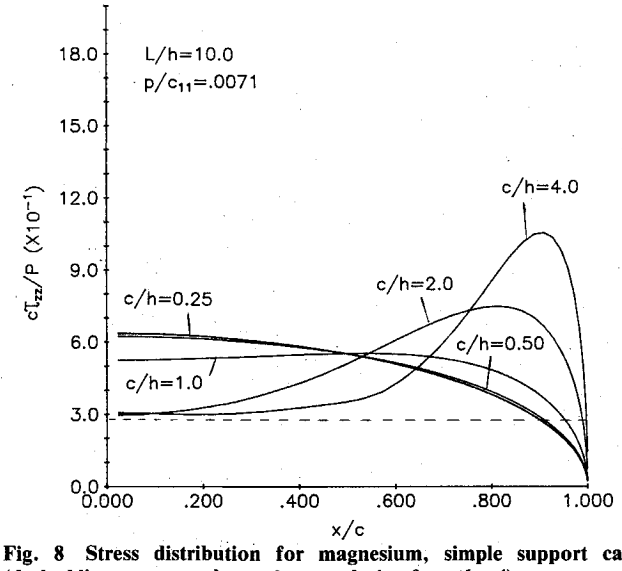

Fig. 8 Stress distribution for magnesium, simple support case (dashed line represents beam theory solution for $c/h = 4$).

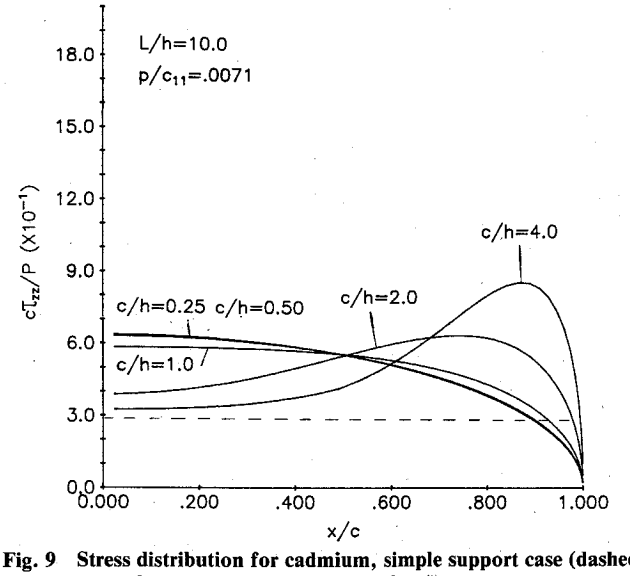

Fig. 9 Stress distribution for cadmium, simple support case (dashed line represents beam theory solution for $c/h = 4$).

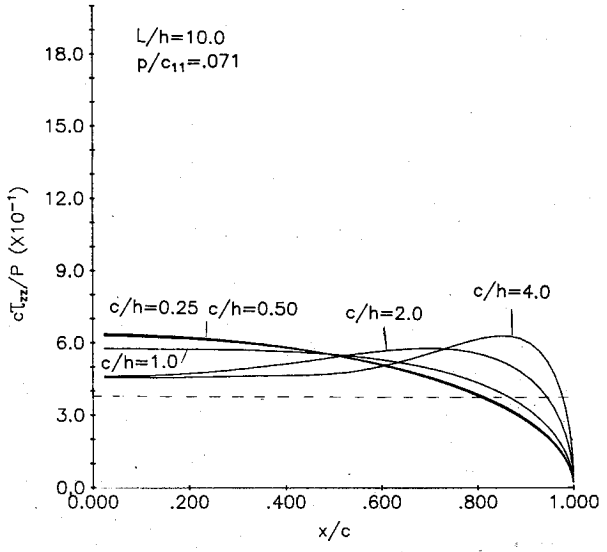

Fig. 10 Stress distribution for magnesium, simple support case (dashed line represents beam theory solution for $c/h = 4$).

correct assumptions in more advanced analyses, such as the problem of impact of composites.

Initial Stress Not Zero

These same calculations were performed for initial stress not equal to zero. The major differences between these cases are in the stress distributions and load deflection relationships. Figures 2 and 3 show that initial stress increases the bending stiffness of the beam. This is due to the fact that the initial stress contributes a bending moment opposite to that due to the transverse loading. The contact stress distributions also differ. From beam theory a constant stress is predicted along the region of contact and, as seen from Figs. 8-10, as c/h increases the elasticity solution does indeed approach a constant value, and this value is lower than that predicted by beam theory. Again we see that magnesium experiences higher peak stresses for most contact lengths. Figure 10 shows that as the initial stress becomes very large, the stress distribution approaches a constant value. This is the same as the distribution predicted by a cable solution.

The overall behavior of the beam can be determined using beam theory, as seen from Figs. 4 and 5. The difference in compliances between elasticity theory and beam theory does not exceed 15%, and this large variation occurs only at the lower aspect ratios. As expected, beam theory predicts a stiffer beam, since the system constraint in beam theory is greater. The details of the beam theory solutions are not given here, but for an account of the theory which includes wrapping see Timoshenko.[9] The results for the clamped case are not given here.

Even though they are not included here, numerical results show that, for the same contact length, magnesium can tolerate a higher load than cadmium. This is due to cadmium being softer in the vertical direction and therefore being more sensitive to the contact. This effect is pronounced as the contact length increases and the aspect ratio decreases. The contact in these cases is due to the punch penetrating into the material and cadmium, being softer, will tolerate a lower load. As the aspect ratio increases, the contact is due to the material wrapping around the punch (a bending effect) and cadmium's softness does not manifest itself as much.

This work can be viewed as a basis for studying the more complicated phenomenon of the impact of composites. The solution of this complex problem may be applied to the analysis and design of such structures as airplane frames, etc. The fact that initial stress is accounted for is significant in that the initial stress can model the membrane stress in an airplane

panel and the contact stresses can model local effects due to the loading.

Acknowledgments

The authors are grateful for support from the National Science Foundation (Grant CME 8006265) and the AFOSR (Grant AFOSR-82-0330).

References

[1] Hill, R., "On Uniqueness and Stability in the Theory of Finite Elastic Strain," *Journal of the Mechanics and Physics of Solids,* Vol. 5, 1967, pp. 229-241.

[2] Dorris, J. F. and Nemat-Nasser, S., "Instability of a Layer on a Half Space," *Journal of Applied Mechanics*, Vol. 47, 1980, pp. 304-312.

[3] Keer, L. M., Nemat-Nasser, S., and Oranratnachai, A., "Surface Instability and Splitting in Compressed Brittle Elastic Solids Containing Crack Arrays," *Journal of Applied Mechanics*, Vol. 49, 1982, pp. 761-767.

[4] Green, A. E., Rivlin, R. S., and Shield, R. T., "General Theory of Small Elastic Deformations Superposed on Finite Elastic Deformations," *Proceedings of the Royal Society* (London), Ser. A., Vol. 211, 1952, pp. 128-154.

[5] Biot, M. A., *Mechanics of Incremental Deformations*, John Wiley & Sons, New York, 1965.

[6] Nemat-Nasser, S., "Continuum Bases for Consistent Numerical Formulation of Finite Strains in Elastic and Inelastic Structures," *Finite Element Analyses of Transient Nonlinear Structural Behavior,* edited by T. Belytschko, J. R. Osias, and P. V. Marcel, ASME, AMD, Vol. 14, 1975, pp. 85-98.

[7] Green, A. E. and Zerna, W., *Theoretical Elasticity*, 2nd ed. Clarendon Press, Oxford, England, 1968, pp. 177-181.

[8] Mowry, D. B. and Keer, L. M., "The Stress Field Created by a Circular Sliding Contact on Transversely Isotropic Spheres," *International Journal of Solids Structures*, Vol. 15, 1979, pp. 33-39.

[9] Timoshenko, S., *Strength of Materials,* Pt. II, Van Nostrand Co., Princeton, N.J., 1930, p. 69.